International Journal of Smart Home
Vol. 10, No. 6 (2016), pp. 221-234
http://dx.doi.org/10.14257/ijsh.2016.10.6.22

TOA Analysis Based on Energy for 60 GHz Signals

Xiao-Lin Liang[1], Hao Zhang[1, 2], Ting-Ting Lu[1], T. Aaron. Gulliver[2]

[1]College of Information Science and Engineering,
Ocean University of China, Qingdao, 266100, China;
[2]Department of Electrical and Computer Engineering,
University of Victoria, Victoria V8W 3P6, Canada
xiaolin87liang@163.com, zhanghao@ouc.edu.cn,
lvtingting33@163.com, agullive@ece.uvic.ca

Abstract

In the field of sensor networks, impulse radio 60 GHz signals are even much more practical for accurate localization which is low cost, low complexity with high time and multipath resolution. Typically, accurate Time of Arrival (TOA) estimation is very important for localization. In order to improve precision of TOA estimation, a new TOA estimation algorithm based on energy detector (ED) is proposed which is based on a joint metric of skewness, standard deviation and kurtosis after ED. The best threshold based on signal-to-noise ratio (SNR) is investigated and effects of integration period and channel model are examined. Simulation results are presented which show for IEEE802.15.3c channel models CM1.1 and CM2.1, the proposed algorithm provides better precision and robustness in both high and low SNR environments than other ED-based algorithms.

Keywords*: 60 GHz, TOA estimation, energy detector, skewness, kurtosis, standard deviation*

1. Introduction

The demand for high data rate wireless communications with low latency has increased dramatically in recent years. Unfortunately, due to spectrum limitations and transmit power regulations, current short-range wireless communication strategies cannot achieve Gigabit per second (Gbps) data rates. Fortunately, wireless communications in 60 GHz millimeter wave band has become viable for Gbps wireless communication networks [1-4] due to availability of several GHz of license-free spectrum, up to 10W maximum transmit power, no interference from other systems, and development of low-cost complementary metal-oxide semiconductor devices. Federal communications commission permits communications in 60 GHz unlicensed band at an effective isotropic radiated power of up to 40dBm, which is many times greater than other short-range wireless communication strategies. In China, this limit is 44dBm [5]. Although path loss is high at 60 GHz, received power can still be significant. Impulse radio communication strategies have been proposed for this frequency band because it can be effective in separating multipath signals at receiver. This is because short pulses are employed for communications with a duration (typically under 100 picoseconds), which is far less than multipath propagation delay. These signals can also provide fine multipath resolution required for high precision ranging and localization [6]. Thus, 60 GHz signals are even much suitable for localization applications for short distances.

Generally, localization strategies can be classified into time based [7-10] and non-time based [11]. For example, TOA [10, 12] and Time Difference of Arrival (TDOA) [10] are range based strategies, while Received Signal Strength (RSS) and Angle of Arrival (AOA) [11] are non-range based. Localization that based on range (TOA or TDOA) is even much

ISSN: 1975-4094 IJSH

suitable for using with 60 GHz strategy [11], as it can take full advantage of higher time and multipath resolution available with very short 60 GHz signals. TOA estimation which is even much more accurate is key to accurate ranging, but this is very challenging due to potentially hundreds of multipath components in 60 GHz channels, even in Non-line of Sight (NLOS) environments.

TOA estimation has been extensively studied [12, 15-18] for past few years. There are two approaches which are much more applicable for TOA estimation, a Matched Filter (MF) [16] (such as a rake or correlation receiver) with a higher sampling rate and higher precision correlation, or ED [18] with a lower sampling rate and lower complex. MF is optimal strategy for TOA estimation, where a correlator template is matched exactly to the received signal. However, a receiver operating at Nyquist sampling rate makes it very difficult to align with multipath components of received signal [15]. In addition, MF requires a priori estimation of channel, including timing, fading coefficient, and pulse shape for each component of impulse response [15]. Because of higher sampling rates and channel estimation, MF may not be practical in many applications. As opposed to a more complex MF, ED is a non-coherent approach to TOA estimation. It consists of a square-law device, followed by an integrator, sampler and a decision mechanism. TOA estimate is made by comparing integrator output with a threshold and choosing the first sample to exceed threshold. This is a convenient strategy that directly yields an estimate of start of received signal. Thus, a low complexity, low sampling rate receiver can be employed without need for a priori channel estimation.

The major challenge with ED is selection of an appropriate threshold based on received signal samples. In [17], a normalized threshold selection strategy for TOA estimation was proposed which exploits kurtosis of received samples. In [18], an approach based on minimum and maximum sample energy was introduced. Threshold selection for different SNR values was investigated via simulation. These approaches have limited TOA precision, as the strongest path is not necessarily the first arriving path.

In this paper, we consider relationship between SNR and statistics of integrator output including kurtosis, skewness and standard deviation. A metric based on kurtosis, skewness and standard deviation is then developed for threshold selection. The threshold for different SNR values is investigated and effects of integration period and channel are examined. Performance results are presented which show that in both CM1.1 and CM2.1 channels, this joint metric provides higher precision and robustness.

The remainder of this paper is organized as follows. In Section 2 system model is outlined. Section 3 discusses various TOA estimation algorithms based on ED. Section 4 considers statistical characteristics of energy values. In Section 5 a joint metric based on kurtosis, skewness and standard deviation is proposed. S

2. System Model

Currently, there are two important standards that have been developed for 60 GHz wireless communications systems, IEEE 802.15.3c and IEEE 802.11ad [19-20]. In this paper, channel models in IEEE 802.15. 3c standard are used because it is specifically designed for wireless personal area networks and thus encompasses typical indoor environments. Further, these are the most widely employed models for 60 GHz systems. IEEE 802.15.3c standard was the first developed for high data rate short-range wireless systems. The physical layer was designed to support transmission of data within a few meters at a minimum data rate of 2 Gbps. These models have been developed for communications in frequency band 57 to 66 GHz in indoor residential, indoor office and library environments (with differences largely due to LOS and NLOS characteristics) [21-25]. In this paper, a pulse position modulation time hopping 60 GHz signal is employed for ranging purposes. The propagation delay $\hat{\tau}$, between transmitter and receiver is estimated for use in localization.

2.1. 60 GHz Signal

The 60 GHz signals have a very short duration (typically 100 picoseconds or less), and can be expressed as:

$$s(t)=\sum_{-\infty}^{\infty} p\left(t-jT_s-C_jT_c-a_j\varepsilon\right) \tag{1}$$

Each symbol is represented by a sequence of very short pulses, where T_s is symbol time. The Time Hopping (TH) code represented by C is a pseudorandom integer-valued sequence which is unique for each user to limit multiple access interference, and T_c is chip time. The PPM time shift is ε so that if a_j is 1, signal is shifted in time by ε, while a_j is 0, there is no shift. In general, these parameters satisfy following relationship:

(1) $C_jT_c+\varepsilon<T_s$; (2) $\varepsilon<T_c$; (3) $a_j\varepsilon<C_jT_c\left(C_j\neq 0\right)$

Many pulse shapes have been proposed for 60 GHz systems. In this paper a Gaussian pulse is employed which is multiplied by carrier signal to give as shown in Figure 1 [26]:

$$p(t)=\frac{\sqrt{2}}{\alpha}\exp\left(-2\pi\frac{t^2}{\alpha^2}\right)\cos\left(2\pi f_c t\right) \tag{2}$$

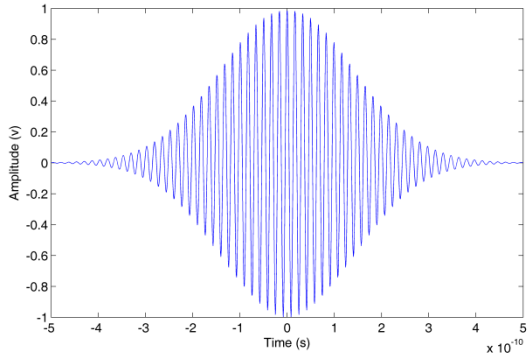

Figure 1. Waveform of 60 GHz Signal

where α is shape factor, and f_c is carrier frequency which here is $f_c=60$ GHz. A smaller shape factor results in a shorter duration pulse and a larger bandwidth.

2.2. Signal Shift and Path Loss

The path loss is defined as ratio of received signal power to transmit signal power and it is very important for link budget analysis. Unlike narrow-band system, path loss for a wide-band system such as mm-wave system is both distance and frequency dependent. In order to simplify the models, it is assumed that frequency dependence path loss is negligible and only distance dependence path loss is modeled. The signal path loss, which depends on propagation distance and channel (IEEE 802.15.3c), is described by:

$$PL(d)[dB]=PL_0+10\cdot n\log_{10}\left(\frac{d}{d_0}\right)+X_\sigma[dB];\ d\geq d_0 \tag{3}$$

where d_0 and d denote reference distance, and distance respectively. n is path loss exponent for mm-wave, X_σ is that unit dB, with mean zero and variance σ_s for a Gaussian random variable [11]. Table 1 summarizes values of n, PL_0, σ_s for different environments and scenarios.

Table 1. Values of n, PL_0 , σ_s for Different Environments and Scenarios

environments	*n*	PL_0	σ_s
Indoor residential(LOS)	1.53	75.1	1.50
indoor residential(NLOS)	2.44	86.0	6.20
indoor office (LOS)	1.16	84.6	5.40
indoor office (NLOS)	3.74	56.1	8.60

The signal shift can be expressed as:

$$t = dt * floor\left(\left(d / c\right)/dt\right) \tag{4}$$

where *d* denote distance between transmitter and receiver, *dt* is sampling period and *c* is speed of light which is 299792458m/s in the air.

2.3. Multipath Fading Channel

The received signal can be written as:

$$r\left(t\right) = \sum_{n=1}^{N} \alpha_n p\left(t - \tau_n\right) + n\left(t\right) \tag{5}$$

where *N* is number of received multipath components, α_n and τ_n denote amplitude and delay of n^{th} path respectively, $p(t)$ is received 60 GHz pulse and $n(t)$ is additive white Gaussian noise with zero mean and two sided power spectral density $N_0/2$. Equation (5) can be rewritten as

$$r\left(t\right) = s\left(t\right) * h\left(t\right) + n\left(t\right) \tag{6}$$

where $s(t)$ is transmitted signal, and $h(t)$ is channel impulse response which can be expressed as:

$$h\left(t,\theta\right) = \sum_{k=1}^{K} \sum_{l=1}^{L_k} \mu_{kl} \delta\left(t - T_k - \tau_{kl}\right) \delta\left(\theta - \theta_k - \omega_{kl}\right) \tag{7}$$

where $\delta(.)$ is dirac-delta function, K is number of clusters, L_k is number of rays in k^{th} cluster, and μ_{kl} , τ_{kl} and ω_{kl} denote complex amplitude, delay and azimuth of k^{th} ray of l^{th} cluster, respectively. Similarly, T_k and θ_k represent delay and mean Angle of Arrival of the k^{th} cluster.

2.4. Energy Detector

As shown in Figure 2 [27], after amplifier, received signals are squared, and then input to an integrator with integration period Tb . Because of inter-frame leakage due to multipath signals, integration duration is $3T_f / 2$, so number of signal values for ED is $N = 3T_f / 2Tb$. The integrator outputs can be expressed as:

$$z\left[n\right] = \sum_{i=1}^{N} \int_{(i-1)T_f + (c_j + n)Tb}^{(i-1)T_f + (c_j + n - 1)Tb} r^2\left(t\right) dt \tag{8}$$

where $n \in \{1, 2, .., N\}$ denotes sample index with respect to starting point of integration period and *N* is number of pulses per symbol. Here, *N* is set to 1, so integrator outputs are

$$z\left[n\right] = \sum_{i=1}^{N} \int_{(c_j + n - 1)Tb}^{(c_j + n)Tb} r^2\left(t\right) dt \tag{9}$$

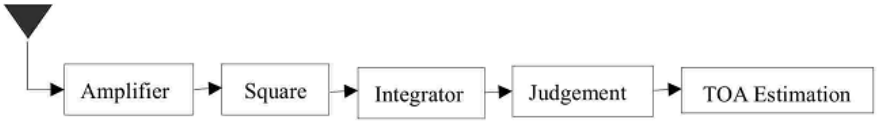

Figure 2. Block Diagram of Energy Detector Receiver

If $z[n]$ is integration of noise only, it has a centralized Chi-square distribution, while it has a non-centralized Chi-square distribution if a signal is present. The mean and variance of noise and signal values are given by [17] respectively.

$$\mu_0 = F\sigma^2, \sigma_0 = 2F\sigma^4 \quad (10)$$

$$\mu_e = F\sigma^2 + E_n, \sigma_e^2 = 2F\sigma^4 + 4\sigma^2 E_n \quad (11)$$

where E_n is signal energy within the n^{th} integration period and F is number of degrees of freedom given by $F = 2BTb + 1$. Here B is signal bandwidth.

3. TOA Estimation Based on Energy Detector

3.1. TOA Estimation Algorithms

There are many TOA estimation algorithms based on ED for determining start block of a received signal. The simplest is Maximum Energy Selection (MES), which chooses maximum energy value to be start of signal value. TOA is estimated as center of corresponding integration period:

$$\tau_{MES} = \left[\arg\max_{1 \le n \le N_b} \{ z[n] \} - 0.5 \right] Tb \quad (12)$$

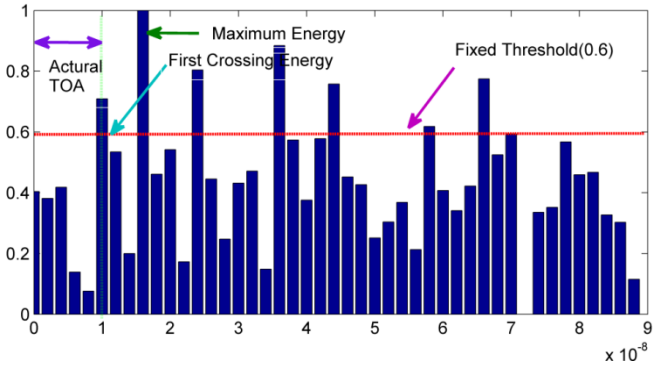

Figure 3. TOA Estimation Based on Energy Detector

However, as show in Figure 3, maximum energy value may not be the first energy block [13], especially in NLOS environments. On average, the first energy value $z[n]$ is located before maximum $z[n_{\max}]$, i.e. $n \le n_{\max}$. Thus, Threshold Crossing TOA estimation has been proposed where received energy values are compared to an appropriate threshold α. In this case, TOA estimation is given by:

$$\tau_{TC} = \left[\arg\min_{1 \le n \le n_{\max}} \{ n \mid z[n] \ge \xi \} - 0.5 \right] Tb \quad (13)$$

It is difficult to determine an appropriate threshold α directly, so usually a normalized threshold α_{norm} is calculated. Using α_{norm}, α is given by:

$$\alpha = \alpha_{norm} \left(\max(z(n)) - \min(z(n)) \right) + \min(z(n)) \quad (14)$$

TOA (τ_{TC}) is then obtained using (11). A simpler Threshold Crossing algorithm is Fixed

Threshold algorithm where threshold is set to a fixed value, for example α_{norm}=0.4 .The problem in this case becomes one of how to set threshold. It should be based on statistics of signal energy, particularly for multipath, NLOS indoor environments.

3.2. Error Analysis

Mean Absolute Error (MAE) of TOA estimation based on Threshold Crossing was analyzed, and closed form error expressions derived. MAE can be used to evaluate quality of an algorithm, and is defined as:

$$MAE = \frac{1}{N}\sum_{n=1}^{N}\left(t_n - t_n\right) \tag{15}$$

where t_n is n^{th} actual propagation time, t_n is n^{th} TOA estimate, and N is number of TOA estimates.

4. Statistical Characteristics

Kurtosis and skewness of the energy blocks are analyzed in this section.

4.1. Kurtosis

Kurtosis is calculated using the second and fourth order moments and is given by:

$$k = \frac{E\left[\left(x_i - \mu_x\right)^4\right]}{E\left[\left(x_i - \mu_x\right)^2\right]^2} = \frac{E\left[\left(x_i - \mu_x\right)^4\right]}{\sigma_x^4} \tag{16}$$

where μ_x is mean value, and σ_x is standard deviation. Kurtosis for a standard normal distribution is three. For this reason, kurtosis is often redefined as $\mathrm{K} = \mathrm{K} - 3$ (often referred to as "excess kurtosis"), so that standard normal distribution has a kurtosis of zero, positive kurtosis indicates a "peaked" distribution and negative kurtosis indicates a "flat" distribution. For noise only (or for a low SNR) and sufficiently large F (degrees of freedom of Chi-square distribution), $z[n]$ has a Gaussian distribution and kurtosis = 0. On the other hand, as SNR increases, kurtosis will tend to increase.

4.2. Skewness

Skewness is given by:

$$S = \frac{1}{(N-1)\delta^3}\sum_{i=1}^{N}\left(x_i - \mu_x\right)^3 \tag{17}$$

where μ_x is mean value, and δ is standard deviation of energy values. Skewness for a normal distribution is 0, in fact any symmetric data will have a skewness of zero. Negative values of skewness indicate that data is skewed left, while positive values indicate data that is skewed right. Skewed left indicates that left tail is long relative to right tail, while skewed right indicates opposite. For noise only (or very low SNR), and sufficiently large F, Skewness is 0. As SNR increases, skewness will tend to increase.

4.3. Maximum Slope

Kurtosis cannot account for delay or propagation time, so slope of energy values is considered as a measure. These values are divided into (N-M+1) groups, with M values in each group. The slope for each group is calculated using a least squares line-fit. Maximum slope can then be expressed as:

$$MS = \min_{1\le n\le N-M+1} slope\left\{linefit\left(z[n], z[n+1], ..., z[n+M-1]\right)\right\} \tag{18}$$

4.4. Standard Deviation

Standard deviation is a widely used measure of variability. It shows how much variation or "dispersion" there is from average (mean or expected value). Standard deviation is given by:

$$D = \sqrt{\frac{\sum_{i=1}^{N}\left(x_i - \mu_x\right)^2}{N-1}} \tag{19}$$

4.5. Characteristics of Parameters

In order to examine characteristics of parameters (skewness, kurtosis and standard deviation), CM1.1 (residential LOS) and CM2.1 (residential NLOS) channel models from IEEE 802.15.3c standard are employed. For each SNR value, 1000 channel realizations are generated and sampled at $f_c = 1 \cdot e^{10}$ Hz. The other system parameters are $T_f = 200ns$, $T_c = 1ns$ Tb is 1ns and 4ns and N = 1. Each realization has a TOA uniformly distributed within $\left(0\, T_f\right)$.The parameters were calculated, and results obtained are shown in Figure 4. Results show that characteristics of parameters with respect to SNR are similar for two channels. The results of division of standard deviation and kurtosis used as new parameter 'SD/K', results of division of skewness and kurtosis used as new parameter 'K/S'. From Figure 4, results show K/S, skewness and kurtosis increases as SNR increases both in CM1.1 and CM2.1, but K/S changes more rapidly in comparison with skewness and kurtosis. Conversely, SD/K decrease with increase of SNR. They better reflect changes in SNR, and so they are even more suitable for TOA estimation. Moreover, when SNR is less than 11 dB, K/S changes slowly while SD/K changes rapidly. On the other hand, when SNR is higher than 11 dB, K/S changes rapidly but SD/K changes slowly. No single parameter is a good measure of SNR change over a wide range of values. Thus, a joint metric based on skewness, kurtosis and standard deviation is proposed in next section for TOA estimation. Based on results above, a joint metric for TOA estimation is formulated as:

$$G = K / S - norm\left(SD / K\right) * n \tag{20}$$

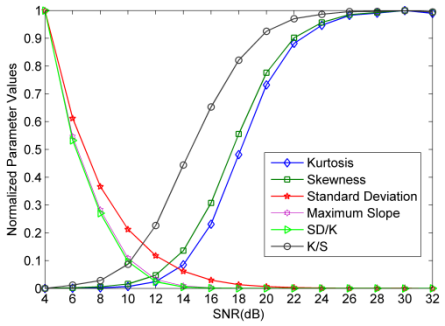

(CM1.1 with Tb = 1ns)

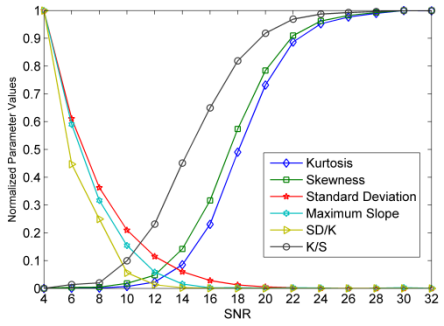

(CM1.1 with Tb = 4ns)

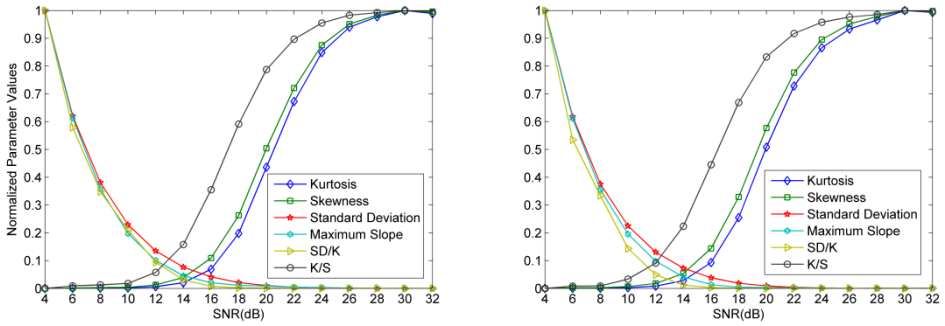

(CM2.1 with Tb = 1ns) (CM2.1 with Tb = 4ns)

Figure 4. Parameters Change with SNR

5. Optimal Threshold Selection

The relationship between *G* and optimal normalized threshold α_{opt} must be established. According to Figure 5, curves for CM1.1 and CM2.1 for a given value of *Tb* are similar, so models are derived only for *Tb*=1ns and *Tb*=4ns.The steps to establish relationship between *G* and α_{opt} can expressed as:

- Generating amounts of channel realizations (1000 channel realizations are generated in this paper) aiming at different channel model (CM1.1 and CM2.1), *Tb* = 1ns and 4ns, and SNR value in range from 4dB to 34dB.
- Calculating average value of MAE with respect to different α_{norm} for different G value, channel model (CM1.1 and CM2.1), and Tb as shown in section"5.2.Relationship between MAE and Normalized Threshold". In process of simulation, because of signals are generated randomly, so there are different MAE values with respect to one normalized threshold, so average MAE is obtained. At the same time, because *G* is a real value, *G* should be rounded to the nearest discrete value, for example integer value or half-integer value.
- Selecting normalized threshold with the lowest MAE as best threshold α_{best} with respect to G for each channel model and Tb, as shown in section "Optimal thresholds".
- Calculating average normalized thresholds of channels CM1.1 and CM2.1 for different G as optimal normalized threshold α_{norm}, as shown in section "Optimal thresholds".

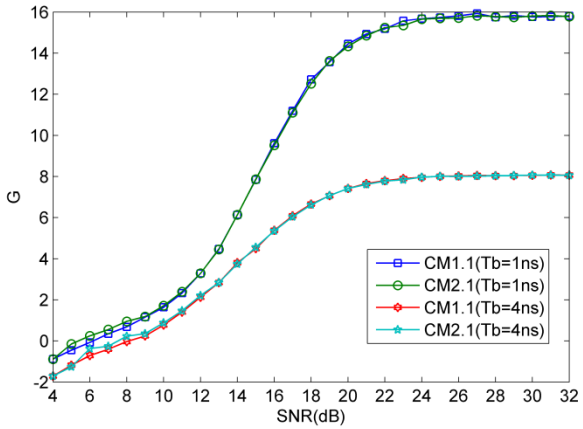

Figure 5. Average Values with Respect to SNR for Different CM and Tb

5.1. Relationship between G and SNR

In order to verify relationship between G and SNR, 1000 channel realizations were generated when SNR is from 4 dB to 34 dB in each IEEE 802.15.3c channel. The average values of G are presented in Figure 5. The results show G is a monotonic function for a large range of SNR values, and it is even much more sensitive to changes in SNR. The fixed curves differ somewhat due to Channel Model and integration period used. The figure shows that G is more sensitive to Tb .

5.2. Relationship between MAE and Normalized Threshold

In order to determine best threshold (α_{best}) based on G, relationship between MAE and normalized threshold (α_{norm}) was investigated. 1000 channel realizations with SNR={4, 5,…, 34} dB were simulated under CM1.1 and CM2.1 environments α is threshold which is compared to energy values to find the first threshold crossing. When α is bigger than $z[n_{\max}]$, we can't get TOA estimation, so in this case, α is set to be 1. In the simulation, all G values were rounded to the nearest integer and half-integer values for all SNR values. Figure 6 show relationship between MAE and normalized threshold in CM1.1 and CM2.1 channels, respectively, with Tb is 1ns and 4ns. The relationship is always that MAE decreases as G increases. Another conclusion is that minimum MAE is lower as G increases. The normalized threshold α_{norm} with respect to minimum MAE is just best threshold α_{best} . The relationship between α_{best} and G will be shown in next section.

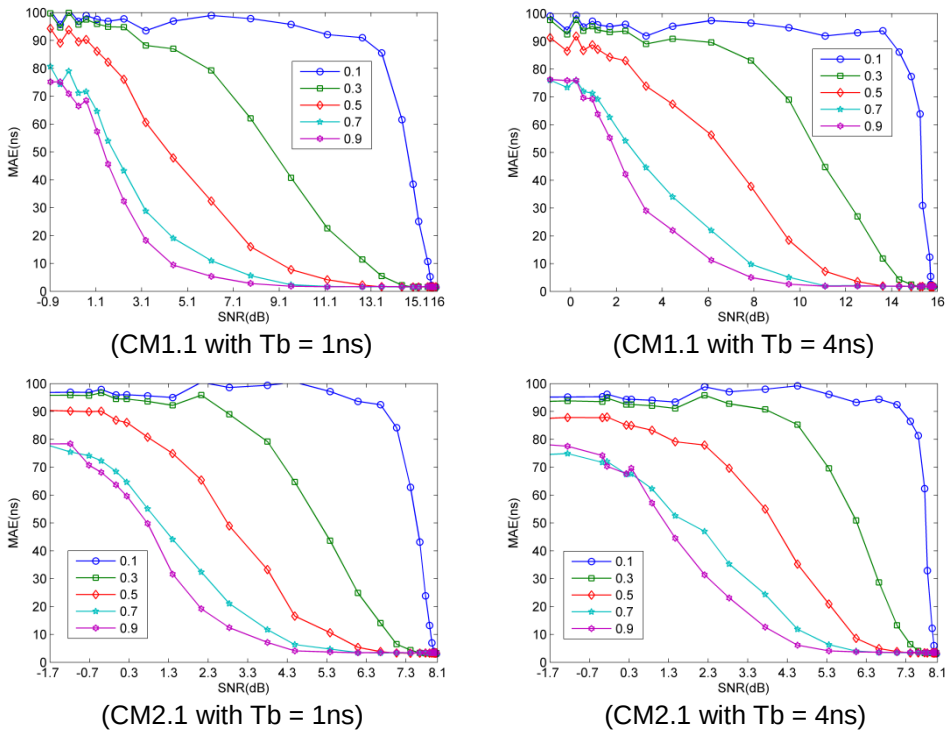

(CM1.1 with Tb = 1ns) (CM1.1 with Tb = 4ns)

(CM2.1 with Tb = 1ns) (CM2.1 with Tb = 4ns)

Figure 6. MAE with Respect to G

5.3. Optimal Thresholds

The normalized threshold α_{norm} with respect to minimum MAE is called the best threshold α_{best} for a given G. Therefore, the lowest points of curves in Figure 6 for each G are selected as α_{best} . These results show that relationship between two parameters is not

affected significantly by channel model, but is more dependent on integration period, so values for channels CM1.1 and CM2.1 can be combined. Therefore, average of two values is used as optimal normalized threshold:

$$\alpha_{opt}^{(Tb=1ns)}(G)=\frac{\alpha_{best}^{(CM1.1,\,Tb=1ns)}(G)+\alpha_{best}^{(CM2.1,\,Tb=1ns)}(G)}{2} \tag{21}$$

$$\alpha_{opt}^{(Tb=4ns)}(G)=\frac{\alpha_{best}^{(CM1.1,\,Tb=4ns)}(G)+\alpha_{best}^{(CM2.1,\,Tb=4ns)}(G)}{2} \tag{22}$$

5.4. Normalized Threshold with G

From results in previous section, relationship between α_{best} and G shows in Figure 7 (1ns) and Figure 8 (4ns) for each value of G. This shows relationship between two parameters is not affected significantly by CM, but is more dependent on integration period. Therefore, piecewise functions were fitted to these results aiming at $Tb=(1ns,4ns)$. The relationship can be described as expression (23), expression (24).

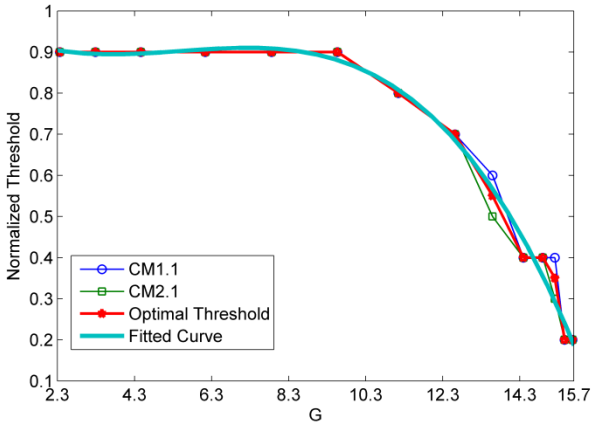

Figure 7. Normalized Threshold with Respect to G (Tb = 1ns)

$$\alpha_{best}=\begin{cases}0.8 & x<2.3592\\ -1.529e^{-6}x^4-6.849e^{-4}x^3+0.01155x^2- & \\ 0.05717x+0.9829 & 2.3592\le x<15.7620\\ 0.1 & 15.6\le x\end{cases} \tag{23}$$

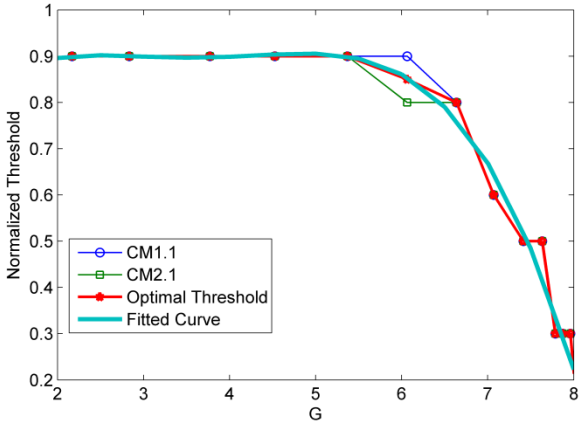

Figure 8. Normalized Threshold with Respect to G (Tb = 4ns)

$$\xi_{best} = \begin{cases} 0.8 & x < 2.1690 \\ 2.431e^{-4}x^5 - 7.694e^{-3}x^4 + 0.07901x^3 - \\ 0.3588x^2 + 0.7445x + 0.3256 & 2.1690 \le x < 8.0337 \\ 0.1 & 8.0337 \le x \end{cases} \quad (24)$$

6. Results and Discussion

In this section, MAE is examined for different TOA estimation algorithms which based on ED in IEEE 802.15.3c CM1.1 and CM2.1 channels. As before, 1000 channel realizations are generated for each case. A 60 GHz signal is employed, and received signal is sampled at $f_c = 1 \cdot e^{10}$ Hz. The other system parameters are $T_f = 200ns, T_c = 1ns$ Tb is 1ns and 4ns and N = 1. Each realization has a TOA uniformly distributed within (0-T_f). MAE for SNR values from 4 dB to 34 dB in LOS (CM1.1) is presented in Figure 9. At the same time, MAE for SNR values from 4 dB to 34 dB in NLOS (CM2.1) is presented in Figure 10. This shows the proposed algorithm performs even much better than other algorithm such as MES and fixed threshold. The performance in CM1.1 is better than in CM2.1 aiming at the same Tb. In most cases, performance with $Tb = 1ns$ is better than that with $Tb = 4ns$ regardless of the channel. MAE performance with three TOA algorithms in channels CM1.1 and CM2.1 are shown in Figures 9-10 respectively.

Here "MES" is Maximum Energy Selection algorithm, and normalized threshold for Fixed Threshold algorithm is set to 0.4 and 0.6. MAE with the proposed algorithm is lower than other algorithms, particularly at low to moderate SNR values. The proposed algorithm is better except when SNR is greater than 19dB. The performance of proposed algorithm is more robust than other algorithms, as performance difference is very small compared to difference with other algorithms. For almost all SNR values the proposed algorithm is even much better. Conversely, performance of other algorithms varies greatly and is very bad for low to moderate SNR values.

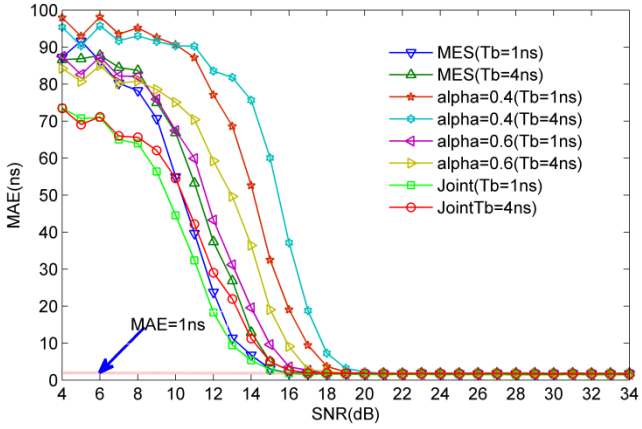

Figure 9. MAE for Different Algorithms with CM1.1 (Tb=1ns and 4ns)

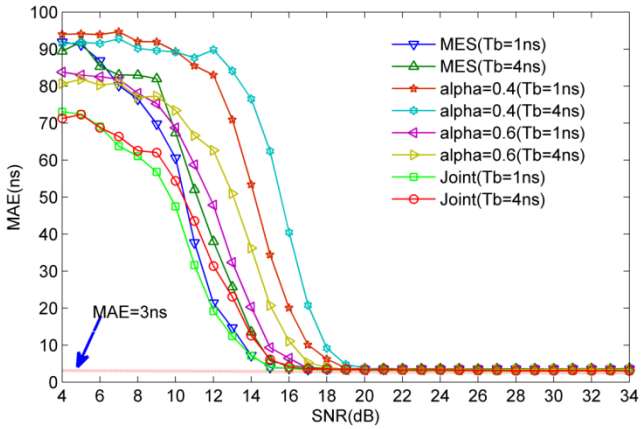

Figure 10. MAE for Different Algorithms with CM2.1 (Tb=1ns and 4ns)

7. Conclusion

Low complex TOA estimation algorithms that based on ED have been examined for 60 GHz ranging, positioning, and tracking applications. Statistical parameters were investigated and a joint metric based on skewness, kurtosis and standard deviation was developed for Threshold Crossing TOA estimation according to results obtained. The best normalized threshold was determined using simulation with CM1.1 and CM2.1 channels. The effects of integration period and channel model were investigated. It was determined that the proposed threshold selection technique is largely independent of channel model. The performance of the proposed algorithm was shown to be better than several known algorithms. In addition, the proposed algorithm is more robust to changes in the SNR and integration period.

Acknowledgments

The authors would like to thank colleagues from UWB Laboratory in College of Information Science and Engineering, Ocean University of China, for help with obtaining measurement data. This work was supported by Nature Science Foundation of China under Grant No. 60902005, Qingdao International Science and Technology Cooperation Projects of Qingdao under Grant No. 12-1-4-137-hz, and Qingdao Transformation of Scientific and Technological Achievements Guiding Plan (youth special program) under Grant No. 14-2-4-37-jch.

References

[1] L. Zhang, "A fully integrated 60GHz five channel CMOS receiver with 7GHz ultra-wide band width for IEEE 802.11ad standard", Communication, China, vol. 11, no. 6, **(2014)**, pp. 42-50.
[2] S. K. Yong and C. C. Chong, "An overview of multi gigabit wireless through millimeter Wave Strategy: Potentials and Technical Challenges", EURASIP J. Wireless Communications and Networking, vol. 2007, no. 1, **(2007)**, pp. 1-10.
[3] R. C. Daniels and R. W. Heath, "60 GHz wireless communications: emerging requirements and design recommendations", IEEE Vehicular Strategy Society, vol. 2, **(2007)**, pp. 41-50.
[4] C. C. Chong, F. M. Peter, Smulders, *et al*, "60GHz-Millimeter-Wave Radio Principle, Strategy, and News Results", EURASIP Journal on Wireless Communications and Networking, vol. 2007, no. 1, **(2007)**, pp. 1-8.
[5] S. K. Yong, P. F. Xia P F and Alberto V G, "60-GHz Strategy for Gbps WLAN and WPAN: From Theory to Practice", Beijing: Press of China Machine, **(2013)**.
[6] R. C. Daniels and R. W. Health, "60 GHz wireless communications: emerging requirements and design recommendations", IEEE Vehicular Strategy Magazine, vol. 2, no. 3, **(2007)**, pp. 41-50.
[7] D. Jie, X. Cui, H. Zhang, and G. Wang, "A ultra-wideband location algorithm based on neural network".

International Conference on Wireless Communications Networking and Mobile Computing (WiCOM), vol. 11, no. 6, (**2010)**, pp. 56-64.
[8] X. Tu, H. Zhang, X. Cui and T. A. Gulliver, "3D TDOA/AOA location based on extended Kalman filter", International Symposium on Antennas, Propagation and EM Theory (ISAPE), vol. 11, no. 6, (**2010)**, pp. 56-64.
[9] Z. Sahinoglu and S. Gezici, "Ranging in the IEEE 802.15.4a standard", in IEEE Wireless and Microwave Strategy Conference (WAMICON), **(2006)**.
[10] D. Dardari, A. Conti, U. Ferner, A. Giorgetti, and M. Z. Win, "Ranging with ultra-wide bandwidth signals in multipath environments", Proceedings of the IEEE, vol. 97, no. 2, (**2009)**, pp. 404-426.
[11] Y. Zhang, A. K. Brown, W. Q. Malik, and D. J. Edwards, "High resolution 3D angle of arrival determination for indoor UWB multipath propagation", IEEE Transactions on Wireless Communications, vol. 7, no. 8, (**2010)**, pp. 3047-3055.
[12] D. Dardari, A. Giorgetti, and M.Z. Win. " Time of arrival estimation of UWB signals in the presence of narrowband and wideband interference", IEEE International Conference on Ultra-Wideband (ICUWB), **(2007)**.
[13] M. Bocquet, C. Loyez, and A. BenlarbiDelai, " Using enhanced TDOA measurement for indoor localization", IEEE Microwave and WireleSG Components Letters, vol. 15, no.10, (**2005)**, pp. 612-614.
[14] A. Abbasi and M.H. Kahaei, "Improving source localization in LOS and NLOS multipath environments for UWB signals". International CSI Computer Conference (CSICC), **(2009)**.
[15] I. Guvenc and Z. Sahinoglu, "Multi-scale energy products for TOA estimation in IRUWB systems", IEEE Global Telecommunications Conference, (GLOBECOM), **(2005)**.
[16] A. Y. Z. Xu, E. K. S. Au, A. K.S. Wong, and Q. Wang, "A novel threshold based coherent TOA estimation for IR-UWB systems", IEEE Transactions on Vehicular Strategy, vol. 58, no. 8, **(2009)**, pp. 4675-4681.
[17] I. Guvenc and Z. Sahinoglu, "Threshold selection for UWB TOA estimation based on kurtosis analysis", IEEE Communications Letters, vol. 9, no. 12, **(2005)**, pp. 1025-1027.
[18] I. Guvenc and Z. Sahinoglu. "Threshold based TOA estimation for impulse radio UWB systems", IEEE International Conference on Ultra-Wideband, **(2005)**.
[19] "IEEE Standard for Information strategy--Local and metropolitan area networks--Specific requirements--Part 15.3: Wireless Medium Access Control (MAC) and Physical Layer (PHY) Specifications for High Rate Wireless Personal Area Networks (WPAN) amendment 2: millimeter-wave-based alternative physical layer extension". IEEE Computer Society, IEEE 802.15.06-0474-00-003c. New York, USA, **(2009)**
[20] "802.11n-2009-IEEE Standard for Information strategy-- Local and metropolitan area networks--Specific requirements--Part 11: Wireless LAN Medium Access Control (MAC)and Physical Layer (PHY) Specifications Amendment 5: Enhancements for Higher Throughput", IEEE Computer Society, IEEE 978-0-7381-6731-2. New York, USA, **(2009)**.
[21] C. R. Andersonn and T. S. Rappaport, "In-building wideband partition loss measurements at 2.5 and 60GHz", IEEE Transactions on Wireless Communications, vol. 3, no. 3, **(2004)**, pp. 922-928.
[22] S. Collong, G. Zaharia and G. E. Zein, "Influence of the human activity on wide-band characteristics of the 60GHz indoor radio channel", IEEE Transactions on Wireless Communications, vol. 3, no. 6, **(2005)**, pp. 2396-2406
[23] A. Maltsev, R. Maslennikov and A. Sevastyanov, "Experimental investigations of 60GHz WLAN systems in office environment", IEEE Journal on Selected Areas in Communications, vol. 27, no. 8, **(2009)**, pp. 1488-1499.
[24] M. G. Sanchez, A. V. Alejos and I. Cuinas, "Comparision of space diversity performance in indoor radio channels at 40GHz and 60GHz", Proc. of European Conference on Wireless Strategy, Amsterdam, **(2008).**
[25] H. B. Yang, "Channel characteristics and transmission performance for various channel configurations at 60GHz", EURASIP Journal on Wireless Communications and Networking, vol. 2007, no. 1, **(2007)**, pp. 43-43.
[26] N. Li, "Study on the properties of 60 GHz impulse radio communication system". Qingdao: Ocean University of China, **(2012)**.
[27] X. Cui, C. Wu and J. Li, "UWB simulation of energy detection algorithm based on the Internet of things", Application of micro-computer, vol, 27, no. 9, **(2011)**, pp.20-26.

Authors

Xiaolin Liang now studies in College of Information Science and Engineering and is a Ph. D. candidate in Ocean University of China. His research interests include ultra-wideband radio systems, 60GHz wireless communication system.

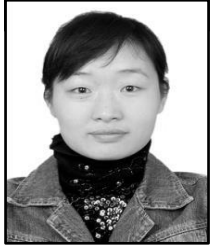

Tingting Lv received Ph. D. degree in College of Information Science and Engineering from Ocean University of China in 2013. She is now a lecture in College of Information Science and Engineering. Her research interests include ultra-wideband radio systems, 60GHz wireless communication system.

Hao Zhang received MBA degree in New York Institute of Technology, American in 2001 and Ph. D. degree in Electrical and Computer Engineering from University of Victoria, Canada in 2004. He was a Project Manager for Microsoft Inc. in United States during January 2000-May 2000. During 2004-2008, he was Vice President for the United States Gamma Capital Inc. He is now an Adjunct Assistant Professor in Department of Electrical and Computer Engineering. Also he becomes a professor and Ph. D. supervisor in College of Information Science and Engineering from Ocean University of China in 2006. His research concerns ultra-wideband radio systems, 60GHz wireless communication system and MIMO wireless communication.

T. Aaron. Gulliver received Ph. D. degree in Electrical and Computer Engineering from the University of Victoria, Canada in 1989. He is now a professor and Ph. D. supervisor in Department of Electrical and Computer Engineering. In 2002, he becomes a Fellow of the Engineering Institute of Canada, and in 2012 a Fellow of Canadian Academy of Engineering. He is also a senior member of IEEE. His research concerns information theory and communication theory, algebraic coding theory and smart grid and ultra-wideband communication.